

Acute White Matter Tract Damage after Frontal Mild Traumatic Brain Injury

Juan J. Herrera,¹ Kurt Bockhorst,¹ Shakuntala Kondraganti,¹
Laura Stertz,² João Quevedo,^{2,3} and Ponnada A. Narayana¹

Abstract

Our understanding of mild traumatic brain injury (mTBI) is still in its infancy and to gain a greater understanding, relevant animal models should replicate many of the features seen in human mTBI. These include changes to diffusion tensor imaging (DTI) parameters, absence of anatomical lesions on conventional neuroimaging, and neurobehavioral deficits. The Maryland closed head TBI model causes anterior-posterior plus sagittal rotational acceleration of the brain, frequently observed with motor vehicle and sports-related TBI injuries. The injury reflects a concussive injury model without skull fracture. The goal of our study was to characterize the acute (72 h) pathophysiological changes occurring following a single mTBI using magnetic resonance imaging (MRI), behavioral assays, and histology. We assessed changes in fractional anisotropy (FA), mean (MD), longitudinal (LD), and radial (RD) diffusivities relative to pre-injury baseline measures. Significant differences were observed in both the longitudinal and radial diffusivities in the fimbria compared with baseline. A significant difference in radial diffusivity was also observed in the splenium of the corpus callosum compared with baseline. The exploratory activity of the mTBI animals was also assessed using computerized activity monitoring. A significant decrease was observed in ambulatory distance, average velocity, stereotypic counts, and vertical counts compared with baseline. Histological examination of the mTBI brain sections indicated a significant decrease in the expression of myelin basic protein in the fimbria, splenium, and internal capsule. Our findings demonstrate the vulnerability of the white matter tracts, specifically the fimbria and splenium, and the ability of DTI to identify changes to the integrity of the white matter tracts following mTBI.

Keywords: diffusion tensor imaging; inflammation; mild traumatic brain injury; MRI behavioral assessments

Introduction

THE CENTERS FOR DISEASE CONTROL AND PREVENTION has estimated that annually 1.7 million people sustain traumatic brain injury (TBI).¹ About 75% of the TBI incidents are classified as mild (mTBI).² mTBI is described as a non-penetrating brain injury induced by traumatic biomechanical forces to the head, neck, or elsewhere on the body that results in physiological disruption of brain function.³ A significant fraction of mTBI survivors live with long-term disabilities that include cognitive impairments, difficulty in concentrating, and headaches that may have a direct negative impact on the quality of life. An understanding of the pathological changes that occur following mTBI and the link between injury and development of psychological disorders is important for discovering new therapeutic approaches.

mTBI typically does not display pathophysiological changes on conventional magnetic resonance imaging (MRI) and computed tomography (CT).^{4–6} mTBI is also thought to transiently disrupt brain

function.^{7,8} A major diagnostic challenge is the visualization of injury and timely identification of the extent of axonal damage following mTBI. Therefore, more sensitive imaging techniques are necessary to identify the subtle tissue pathological changes in the acute phase of injury. A number of studies have demonstrated the presence of lesions on more advanced MRI techniques such as diffusion tensor imaging (DTI).⁹ DTI is based on the microscopic Brownian motion of water within tissues, where water displacement distances are comparable to the cell dimensions.¹⁰ DTI can thus be used to quantify the microstructural changes occurring to the white matter. In DTI, the degree and directionality of water diffusion (anisotropy) can provide information about the integrity of white matter tracts. DTI has been used to examine white matter tract changes following mTBI in patients.^{5,11–13} A number of useful rotationally invariant measures can be derived from the DTI. These include fractional anisotropy (FA) and radial (RD), longitudinal (LD), and mean (MD) diffusivities.

A proper understanding of the pathophysiological and behavioral deficits requires systematic investigation of appropriate

¹Department of Diagnostic and Interventional Imaging, ²Translational Psychiatry Program, Department of Psychiatry and Behavioral Sciences, ³Center of Excellence on Mood Disorders, Department of Psychiatry and Behavioral Sciences, The University of Texas Health Science Center at Houston (UTHealth), McGovern Medical School, Houston, Texas.

experimental models of mTBI. The majority of the published mTBI animal models have limitations that include poor reproducibility and need for craniotomy that make them less relevant to human mTBI.¹⁴ For example, the commonly used models of experimental mTBI such as fluid percussion or controlled cortical impact may result in pathological changes and may not reflect a mild injury because a craniotomy is required.^{15–17} Thus more appropriate closed head TBI models have been developed that have clinically relevant features such as blood–brain barrier breakdown, neurological impairment, and diffuse axonal injury.^{18–20} The Marmarou's impact acceleration model is a weight drop model that mimics diffuse TBI in humans with the force delivered dorsally producing dorsal-ventral linear acceleration.²⁰ The drawback of Marmarou's model is the high variability in injury severity. Also, this closed head TBI model does not specifically reproduce the injury forces encountered by the human brain involved in motor vehicle and sports accidents.²¹ The Maryland closed head TBI model reproduces the acceleration forces frequently encountered by the human brain involved in motor vehicle, sports, and other type of head traumas where frontal impact is combined with lateral rotation of the head reflecting the combinations of anterior-posterior linear acceleration plus sagittal rotational acceleration.²¹

A major focus of the current study is to further characterize the Maryland model examining the acute changes in brain following frontal mTBI using multi-modal MRI, particularly DTI, neurobehavioral, histological, and cytokine expression patterns in white matter tracts.

Methods

Animals and mild traumatic brain injury procedure

The protocol used in this study was reviewed and approved by the Institutional Animal Welfare Committee. The guidelines provided in the National Institute of Health (NIH) Guide for the Care and Use of Laboratory Animal²² were strictly followed.

A total of 30 adult male Sprague Dawley rats weighing between 280 and 300 g were used in this study. The animal breakdown for the study was as follows: 12 animals were used for MRI scans paired with histology and 12 animals (6 injured and 6 uninjured) were used for cytokine measurements. Six animals were used as control for histology. TBIs were produced as described previously.²¹ Briefly, animals were anesthetized with a mixture of 2% isoflurane, air, and oxygen, administered through a Harvard rodent ventilator (Model 683, Harvard Apparatus, Holliston, MA) during the entire procedure. The malar process on each side was exposed via infraorbital incisions. The grooves of the brass rods of the coupling arm were positioned on the malar processes. The energy for the frontal impact was applied via a steel ball (~500 g) accelerated by gravity by rolling down from a vertical height of 2.1 m. The path of the rolling ball was directed by a pair of parallel rails (two pieces of 19-mm diameter tubular steel electrical conduit, joined 3 cm apart at their centers by nuts and bolts) bent to resemble the shape of hockey sticks. After injury the infraorbital incisions were sutured and closed. Animals had free access to food and water.

Magnetic resonance imaging following mTBI

All MRI scans were performed prior to mTBI (baseline) and 72 h after injury. The MRI studies were carried out on a 7T Bruker Biospec 70/30 URS scanner (Bruker, Karlsruhe, Germany). A vendor-supplied birdcage radiofrequency (RF) coil (Bruker) with a 72-mm internal and 112-mm outer diameter was used for transmission. A two-element phased array coil (Bruker) was placed over the head of the animal, which was fixed using ear and mouth bars attached to a PMMA acrylic glass® (polymethyl-methacrylate) animal bed (Bruker). The animal's vital signs were monitored using

a Small Animal Instruments unit (SAI, Stony Brook, NY). It provided readings of the pulse and blood oxygen level via a pulse oximeter (hindpaw clamp), core temperature via a rectal probe, and respiratory movement via a pressure sensor located under the animal. The core temperature was registered and maintained by a feedback-controlled flow of warm air with the SAI module.

Prior to each study, a cylindrical phantom (2.9 cm o.d.) containing deionized water doped with CuSO₄ and NaCl was used to measure the signal-to-noise ratio (SNR) with the macro Auto_SNR, which is a part of the scanner operating system (Bruker, Billerica, MA). In this method the average signal intensity of an array of 3×3 voxels around the brightest voxel was divided by the average of the noise's standard deviation (SD; corners of image) in a single slice using the procedure described elsewhere.²³

For visualizing possible anatomical lesions, images were obtained using the dual echo 2D rapid acquisition with relaxation enhancement (RARE) sequence with the following parameters: number of slices=85, slice thickness=0.3 mm, field of view (FOV)=30 mm×30 mm, matrix=200×200, in plane resolution 0.15×0.15 mm, voxel size 0.00675 mm³, effective echo times (TEs)=29 msec and 79 msec, repetition time (TR)=9245 msec, Hermite pulse, RARE factor=5, bandwidth=50 kHz, number of dummy scans=2, number of averages=4, fat suppression on. The total scan time was 24 min, 40 sec.

For registration and spatial normalization for group analysis, 3D RARE scan matching mostly the geometry of the 2D RARE acquisition was also recorded. The geometric parameters were 0.3 mm×0.3 mm×0.3 mm voxel size, 30 mm×30 mm×25.5 mm FOV, and a 100×100×85 matrix. The other parameters were TR=1000 msec, effective TE=63.7 msec, RARE factor 16, use of fat suppression and saturation slices (*n*=6). The acquisition time was 8.5 min.

The geometry of the DTI protocol was identical to that of the 3D RARE protocol (0.3-mm isotropic voxel size). The data were acquired with a segmented (two shots) 3D echo planar imaging (EPI) sequence, using an icosahedral encoding scheme with bipolar gradients along 42 encoding directions²⁴, TE=24.7 msec, TR=350 msec, Hermite excitation RF pulse (pulse width=2.16 msec, flip angle=90 degrees), bandwidth=247 kHz, number of averages=1, and partial Fourier transform (FT) acceleration=1.5. The diffusion parameters were b-value=800 sec/mm², diffusion gradient duration=4 msec, diffusion gradient separation=8.5 msec, and number of repetitions without any diffusion gradient (*b*₀images)=9. Fat suppression and outer volume suppression (*n*=6) were activated. The acquisition included double sampling, automatic trajectory measurement, and regridding based on the trajectory. The total scan time was 50 min.

MRI analysis

DTI analysis was performed as described previously.^{23,25} Briefly, following the stripping of extra meningeal tissues the diffusion-weighted images (DWI) were smoothed using the procedure described by Hahn and colleagues.²⁶ Initially voxel-wise analysis was performed to identify possible regions that showed significant group differences in the DTI measures. For this purpose all the DWI volumes were registered to one of the volumes that had the best SNR. The registration was performed using the 3D model 4 (105 parameters) of AIR 5.2²⁷

The t-maps showing the regions with significant group differences were then generated with Statistical Parametric Mapping (SPM 8).²⁸ This was followed by region-of-interest (ROI) analysis over the regions that showed significant differences on the t-maps. The ROI analysis was performed in the native space.

Cytokine measurement and histological analysis

The expression levels of cytokines, chemokines, and growth factors were evaluated and measured from the following brain

white matter tract regions: splenium (scc), genu (gcc), fimbria (fi), and internal capsule (ic) using Bio-Plex Pro Rat Cytokine, Chemokine, and Growth Factor Assay Kits (Bio-Rad, Hercules, CA). Briefly, samples were homogenized in a lysing solution containing Protease Inhibitor Cocktail (Sigma), frozen at -70°C overnight. The samples were then thawed, sonicated, and centrifuged at $4500\times g$ for 4 min. The supernatants were collected and total protein concentration was determined using Pierce™ BCA Protein Assay Kit (Thermo Scientific). The following cytokines were assayed: eotaxin, fractalkine, tumor necrosis factor- α (TNF- α), granulocyte colony stimulating factor (G-CSF), granulocyte macrophage (GM-CSF), GRO/KC, interferon gamma (IFN- γ), interleukin (IL)-1 α , IL-1 β , IL-2, IL-4, IL-5, IL-6, IL-10, IL-12 (p70), IL-13, IL-17A, IL-18, inducible protein (IP)-10, leptin, LIX, monocyte chemoattractant protein (MCP)-1, macrophage inflammatory protein (MIP-1 α), MIP-2, regulated upon activation of normal T-cell expressed and presumably secreted (RANTES), and vascular endothelial growth factor (VEGF).

Histological analyses of mTBI and control brains were performed as described previously.^{23,25,29} Briefly, following the MRI scan, animals were transcardially perfused with saline followed by 4% paraformaldehyde in 0.1 M phosphate buffered saline (PBS). The brains were sectioned at $20\mu\text{m}$ thickness and six brain sections/animal were used for staining with each primary antibody: myelin basic protein (MBP, 1:1000; Covance, CA), neurofilament heavy (NF-H, 1:1000; Millipore, Billerica, MA), Iba-1 (1:1000; DAKO), and glial fibrillary acidic protein (GFAP, 1:1000, DAKO). Primary antibodies were diluted with blocking solution (0.1 M PBS containing 5% goat serum and 0.3% Triton X-100). Appropriate secondary antibodies were used at a dilution of 1:600 in 0.1 M PBS.

All images were captured using a Nikon Eclipse Ni-E microscope (Nikon Instruments, Melville, NY). Analysis was performed as described previously.^{23,25,29} Briefly, the exposure times were determined for each antibody in pilot experiments. The threshold levels were set to match those with positive staining and excluded background fluorescence. Image-Pro Plus Software (Media Cybernetics, Inc., Silver Springs, MD) was used to measure the percent areas of fluorescent intensity of the expression of the various antibodies. A circular ROI of $700\mu\text{m}$ size was placed in the regions defined by the DTI analysis and the same ROI size was maintained throughout the experiment. The intensity levels were determined from normal brain sections and the same threshold levels were used on all sections.

Neurobehavioral assessments

Exploratory behavior that included fine motor movements, ambulation, and rearing activities was assessed using Open Field Apparatus (OFA).³⁰ In this assay animals were placed in the activity chambers for a 25-min testing period, and data were collected using the software provided with OFA (Med Associates, Inc., St. Albans, VT). The OFA acquires data on the animal's movements within the activity chamber by recording the number of photo beams interrupted. The activity can be categorized as fine motor movements, gross movements, and rearing. Baseline monitoring was performed before mTBI and 72 h post-injury prior to MRI scans. This assay was performed at approximately the same time of day for both baseline and 72 h post-injury. Rats were allowed to habituate for 30 min prior to each test. Locomotor activity was collected as ambulatory distance traveled or cumulative time associated with four standard behaviors: ambulatory or vertical movement, resting, and stereotypic behavior, measured as repeated breaking of the same photo beam.

Statistical analysis

Comparison between injured and baseline measures for MRI and neurobehavioral assessments were performed using a paired *t* test. Cytokine, chemokine, and growth factor measures and histological

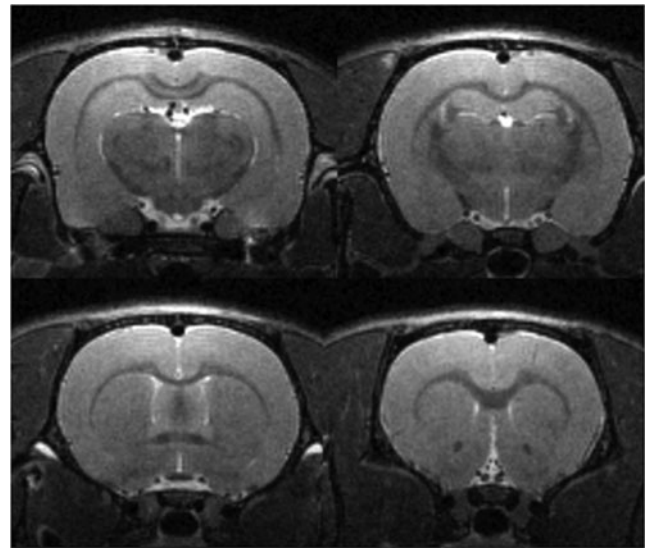


FIG. 1. Coronal rapid acquisition with relaxation enhancement (RARE) images at four different levels of a mild traumatic brain injury (mTBI) animal acquired at 72 h post-mTBI. The acquisition parameters are voxel size $.15\text{ mm}\times.15\text{ mm}\times.03\text{ mm}$; effective echo time (TE)=29 msec, repetition time (TR)=9245 msec. The total scan time is 24 min 39 sec. No anatomical lesions were observed at any level following injury.

measures were compared using unpaired *t* test. Pearson's correlation coefficients between MRI measures, cytokine measurements, histological results, and behavioral results were calculated. The data were analyzed using GraphPad Prism 6 software (GraphPad Software, San Diego, CA).

Results

MRI analysis

The T2-weighted RARE images acquired at 72 h post-injury indicated no observable pathological changes (i.e., lesions, edema; Fig. 1). A representative RGB FA color map of 72 h post-injury brain in the coronal plane is shown in Fig. 2. The red, green, and

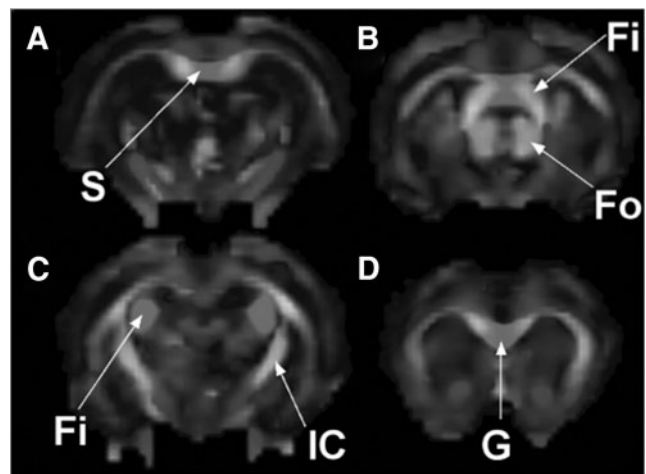


FIG. 2. Fractional anisotropy (FA) maps in a 72 h post mild traumatic brain injury (mTBI) animal at four different sections. Fi, fimbria; Fo, forntix; G, genu; IC, internal capsule; S, splenium.

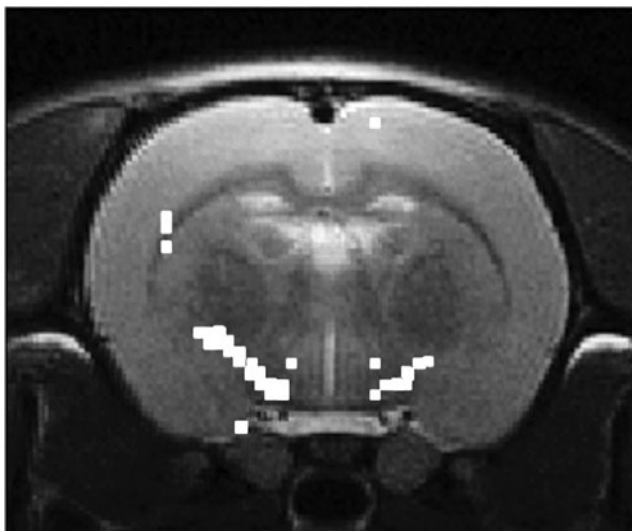


FIG. 3. t-maps showing significant differences in the fractional anisotropy (FA) values between, 72 h post mild traumatic brain injury (mTBI), and sham controls. The t-maps are superimposed on the anatomical image.

blue colors in this figure represent the principle eigenvalue orientations along the left-right, anterior-posterior, and inferior-superior directions, respectively.

The t-maps based on the group analysis indicated significant differences ($p=0.05$; not corrected for multiple comparisons) between baseline and 72 h post-injured scans in the internal capsule (Fig. 3).

Changes in the DTI measures between baseline and 72 h post-injury were calculated by the ROI analysis. ROI placement was guided by the t-maps as described previously.²⁵ The ROIs were placed in the ic, fi, and the corpus callosum (cc). Even though the t-maps did not show significant differences in the gcc and scc of the cc, we included these structures in the ROI analysis because a published study showed differences in the cc following mTBI.³¹ The results from the DTI measures are presented in Table 1. DTI

measures indicated significant increases in FA from the fi and ic region. A significant decrease in LD was observed in the gcc and fi, whereas a significant increase was observed in the RD measures of the fi and scc. An increasing trend in RD was observed in the ic and gcc. No other significant changes or trends were observed in other DTI metrics in the other brain regions.

Histological analysis

Histological analysis was performed on brain sections from the regions analyzed for the DTI measures. Figure 4 shows the splenium region from control (Fig. 4A,C) and mTBI (Fig. 4B,D) brain sections. Quantification of MBP expression indicated significant decrease in the ic ($p=0.0001$), scc ($p=0.002$), and fi ($p=0.0016$). No significant differences were observed in the percent expression of GFAP, and NF-H in the ic, fi, scc, and gcc genu. Also observed in the scc was an increasing trend in the expression of Iba-1 ($p=0.0577$), an indication of the microglial response to injury. No significant difference in the expression of Iba-1 was observed in the ic or fi.

Cytokine measurements

Multiplex assays of uninjured and injured brain samples were processed 72 h post-mTBI. The scc, gcc, ic, and fi were isolated and processed. The results indicated a significant increase in the expression of IL-4 ($p=0.029$), IL-12 ($p=0.050$), and an increasing trend in the expression of RANTES ($p=0.055$) in the scc (Fig. 5). No significant changes were determined in the ic, fi, and gcc regions.

Neurobehavioral assessments

Exploratory behavior results indicated a significant decrease in the average velocity ($p=0.0037$), ambulatory distance ($p<0.0001$), stereotypic counts ($p<0.0001$), vertical counts ($p<0.0001$), ambulatory episodes ($p<0.0001$), and total velocity ($p=0.0004$; Fig. 6). No significant change was observed in the ambulatory counts. The results suggest that the injured animals explored the environment less than baseline control measures.

TABLE 1. DTI METRICS COMPARISON BETWEEN BASELINE AND 72 H POST-INJURY MEASURES

DTI measures	Treatment	White matter structures			
		scc	ic	gcc	fi
FA (dimensionless)	Baseline	0.6895 ± 0.0304	0.5151 ± 0.0356	0.7402 ± 0.04778	0.7325 ± 0.0370
	mTBI	0.6869 ± 0.0360 $p=0.8460$	0.6531 ± 0.0281 $p=0.0001^*$	0.7508 ± 0.0260 $p=0.5685$	0.7757 ± 0.0210 $p=0.0006^*$
MD ($\text{mm}^2 \text{s}^{-1} \times 10^{-6}$)	Baseline	1089 ± 21.06	885.7 ± 65.63	948.1 ± 75.08	944.3 ± 64.63
	mTBI	1368 ± 28.57 $p=0.0063^*$	928.5 ± 82.52 $p=0.2066$	938.3 ± 64.44 $p=0.5089$	870.4 ± 62.07 $p=0.0047^*$
LD ($\text{mm}^2 \text{s}^{-1} \times 10^{-6}$)	Baseline	1659 ± 195.8	1369 ± 117.8	1559 ± 332.3	1672 ± 391.3
	mTBI	1683 ± 279.5 $p=0.7490$	1300 ± 150.9 $p=0.0922$	1293 ± 189.7 $p=0.0179^*$	1289 ± 339.7 $p=0.0069^*$
RD ($\text{mm}^2 \text{s}^{-1} \times 10^{-6}$)	Baseline	589.9 ± 337.3	644.3 ± 138.6	642.7 ± 232.6	580.2 ± 109.1
	mTBI	121.1 ± 331.0 $p=0.0039^*$	742.7 ± 128 $p=0.0849$	762.2 ± 104.4 $p=0.0648$	661.1 ± 88.71 $p=0.0375^*$

*regions showing statistical difference between groups.

DTI, diffusion tensor imaging; FA, fractional anisotropy; LD, longitudinal diffusivity; MD, mean diffusivity; mTBI, mild traumatic brain injury; RD, radial diffusivity.

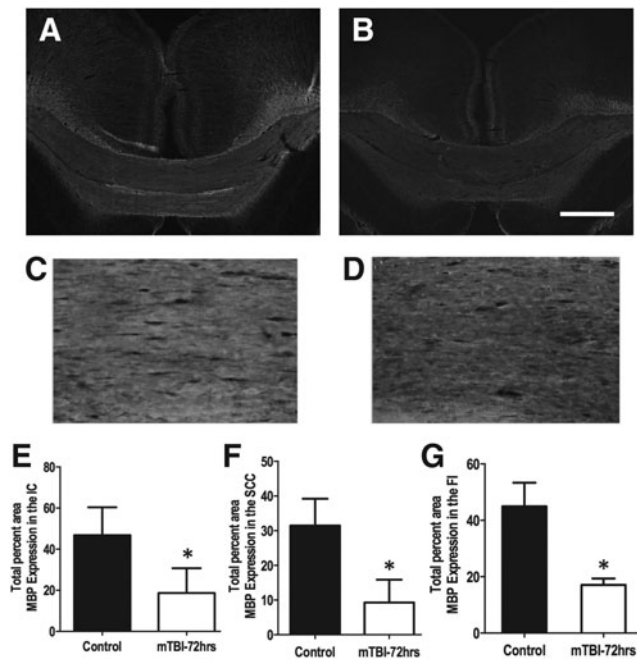


FIG. 4. A representative image of the splenium region from control (A) and injured (B) brain sections showing myelin basic protein (MBP) expression. Higher magnification images of the splenium region from control (C) and 72 h post mild traumatic brain injury (mTBI) (D) used to quantify MBP expression. The 4× and 20× images captured used the same exposure time. Quantification of the expression of MBP indicated a significant decrease in the internal capsule (E), splenium (F), and fimbria (G). A significant decreased in MBP expression is observed in splenium 72 h after injury compared with controls. Scale bar is 500 μm (B). Error bars represent standard deviation.

Relationship between MBP, cytokine measurements, and regional DTI

To determine whether there is a relationship between MBP expression, cytokine measurements, and DTI measures a Pearson’s correlation analysis was performed. The analysis indicated a negative correlation between MBP expression and the splenium FA in mTBI FA ($r = -0.7787, p = 0.0228$). Our analysis also indicated a negative correlation between splenium FA and the following neurobehavioral assessments: average velocity ($r = -0.8453, p = 0.0010$), ambulatory distance ($r = -0.6552, p = 0.0287$), ambulatory counts ($r = -0.6562, p = 0.0283$), stereotypic counts ($r = -0.6885, p = 0.0192$), vertical counts ($r = -0.6088, p = 0.046$), ambulatory episodes ($r = -0.6736, p = 0.0231$), and total velocity ($r = -0.6981, p = 0.0169$). A negative correlation was also determined between fimbria FA and the following behavioral measures: average velocity ($r = -0.8419, p = 0.0012$), stereotypic counts ($r = -0.6439, p = 0.0325$), and total velocity ($r = -0.6583, p = 0.0276$).

Cytokine differences between injured and control tissues were only determined in splenium region of the cc. A significant negative correlation was determined between RANTES expression and MD ($r = -0.8248, p = 0.0434$), LD ($r = -0.8402, p = 0.0363$), and RD ($r = -0.8123, p = 0.0495$).

Discussion

It is of critical importance to gain a true understanding of the pathophysiological and behavioral changes occurring following an

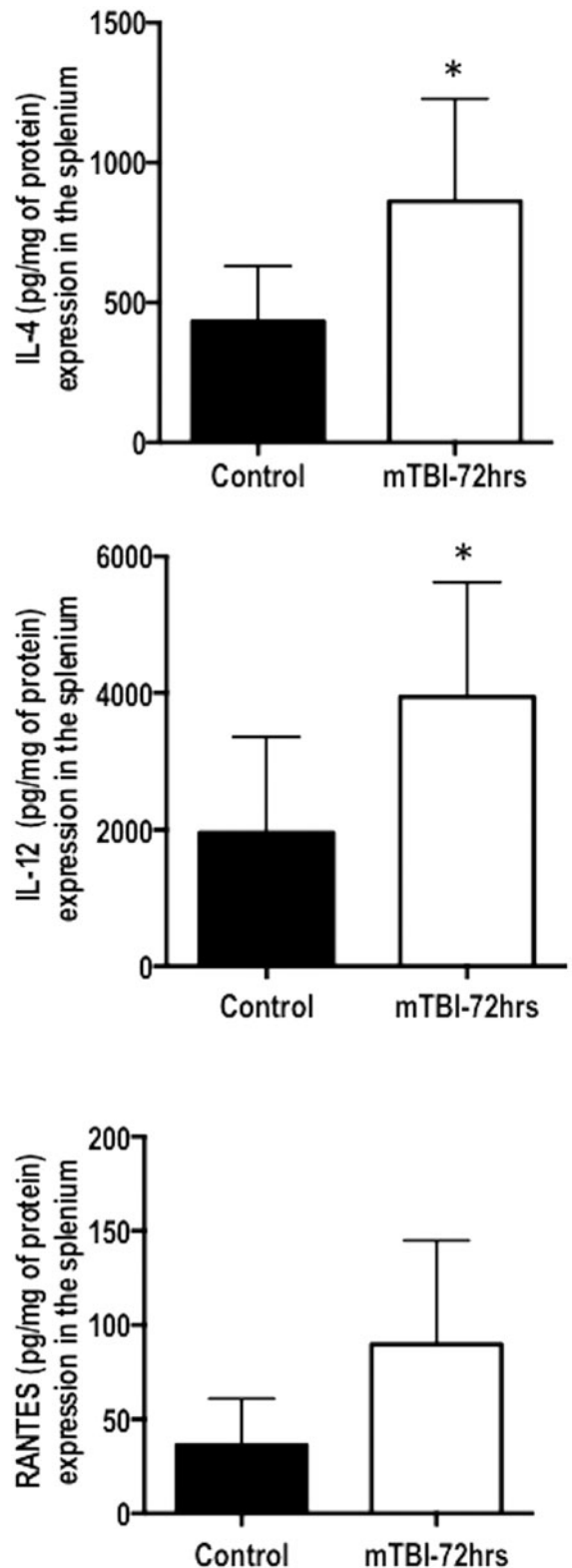


FIG. 5. Multiplex cytokine quantification of 72 h post mild traumatic brain injury (mTBI) compared with naïve controls. The regions examined were the genu, fimbria, internal capsule, and splenium. Only in the splenium was a significant change detected in the cytokines interleukin 4 (IL-4) and IL-12. A significant trend was also detected in the protein RANTES (regulated upon activation of normal T-cell expressed and presumably secreted). Error bars represent standard deviation.

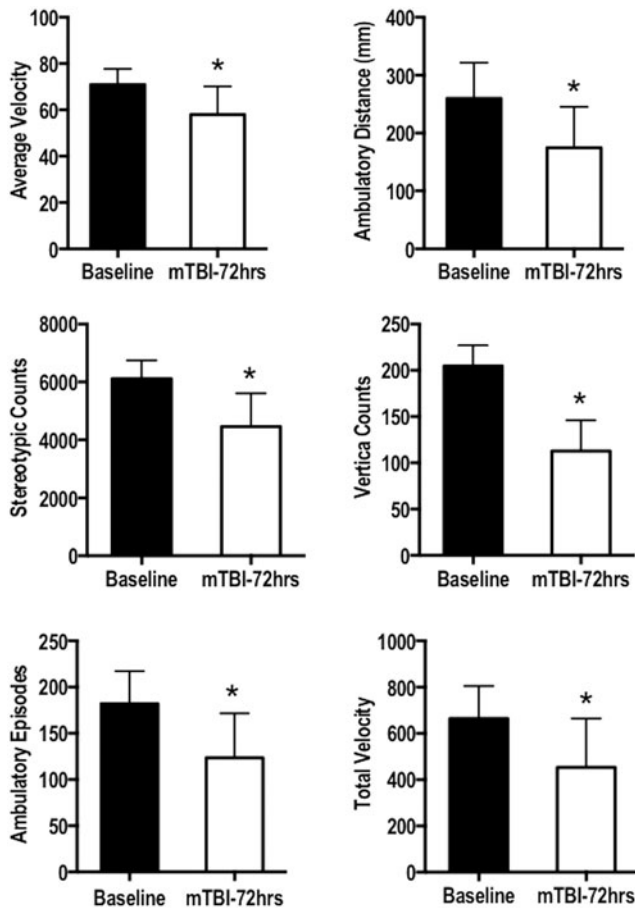


FIG. 6. The exploratory behavior was quantified of 72 h post mild traumatic brain injury (mTBI) animals relative to baseline measures. A paired *t* test indicated a significant difference in the average velocity ($p=0.0037$), ambulatory distance ($p<0.0001$), stereotypic counts ($p<0.0001$), vertical counts ($p<0.0001$), ambulatory episodes ($p<0.0001$), and total velocity ($p=0.0004$). Error bars represent standard deviation.

mTBI for rational-based intervention. Pre-clinical studies examining these changes need to incorporate mTBI models that truly reflect the features observed in human patients.⁷ These features in human mTBI include altered DTI parameters in the acute phase, absence of anatomical lesions on conventional neuroimaging, and behavioral changes (sensory, motor, and cognitive deficits and neuropsychiatric disorders) that may or may not be transient. The current study examined the acute changes in white matter tracts following frontal-delivered mTBI. Our results indicate that when the mTBI is frontally delivered no observable anatomical changes are detected using conventional MRI; however, altered DTI measures were observed, both of which are consistent with characteristics observed in human mTBI.³² The study also indicates changes in the expression of proinflammatory cytokines and behavioral changes following injury. Finally, the current study shows that the Maryland closed head TBI model,²¹ which does not involve a craniotomy, replicates many of the features seen in human mTBI.

The DTI results indicate microstructural alterations as reflected by changes in FA, LD, and RD at 72 h post-injury. These changes are mainly confined to fi and scc, which are long white matter tracts that are reported to be more vulnerable to damage from rotational forces.^{9,33,34} Also observed was a significant decrease in the LD

measure in the gcc and fi. This would suggest a compromise in axonal integrity. Histological analysis indicated a significant decrease in the expression of myelin basic protein in the ic, fi, and the gcc and scc of the cc. The observed demyelination correlates with increased RD. Demyelination has been suggested to reflect an increase in RD.³⁵ Previous studies have demonstrated that following trauma, diffuse axonal injury, or wallerian degeneration, RD increases as a consequence of demyelination.^{5,36,37} The cellular basis for alterations in RD and LD is still not completely understood as there may be other cell populations contributing to the DTI metrics.^{23,25,38} We observed no significant difference in the astrocytic response based GFAP expression in the DTI regions analyzed. Similar observations were made on Western analysis of brain tissue following controlled cortical impact at 3 and 24 h post-injury.³⁹ We recognize that the cellular responses occurring before the 72 h period is likely contributing to the observed changes.

The cytokine and chemokine expression analysis indicated a significant increase in the expression of IL-4 and IL-12 only in the splenium of the cc. IL-4 is a proinflammatory cytokine that regulates the phenotype of meningeal myeloid cells and has a direct effect on astrocytes in inducing the production of brain-derived neurotrophic factor (BDNF), a protein responsible for growth, plasticity, and survival of neurons.^{40,41} This may be consistent with our histological observation of no change in NF-H expression. Previous studies have indicated that IL-4 has a profound effect on cognition, when examined in IL-4 knockout mice.^{42,43} The increase trend in the expression of Iba-1, a marker for microglia, concomitant with the significant increase in IL-4 may indicate a neuroprotective mechanism. For example, it was shown that microglia expressing IL-4 exerts a neuroprotective effect by decreasing the expression of TNF- α and IGF-2.⁴⁴ We observed no significant difference in the expression of TNF- α 72 h after injury in any of the regions examined. TNF- α has been previously demonstrated to be upregulated at less than 24 h after injury.⁴⁵⁻⁴⁷ TNF- α was shown to be cytotoxic to oligodendrocytes.⁴⁸ The increased expression of TNF- α observed during the first 3 to 6 h post-injury induces demyelination and oligodendrocyte apoptosis.⁴⁹ This is in line with a significant decrease in the MBP expression that we observed. The other cytokine, IL-12, also upregulated 72 h post-injury, and is also a proinflammatory cytokine that is implicated in the differentiation of CD4⁺ T cells into inflammatory (T_H1) T cells, activation of CD8⁺ T cells, natural killer (NK) and lymphokine activated killer (LAK) cells, and stimulation of activated T and NK cell proliferation.⁵⁰⁻⁵² The expression profile of IL-12 appears to be TBI model-dependent. A study by Redell and associates indicated a significant decrease of IL-12 at 3 and 24 h after injury using a fluid percussion model, but no significant change in a controlled cortical impact model.³⁹ Another study showed significant increase in IL-12 levels in the cerebrospinal fluid in human TBI patients.⁵³ The increase in IL-12 expression may likely be attributed to an increase in microglia in the splenium. We speculate that the lack of increases in these proinflammatory cytokines in other brain regions that showed a significant increase in microglia labeling may be attributed to the post-injury temporal window at which we examined these proteins.

Spontaneous exploratory behavior was also assessed and a significant decrease was observed in the following measures: average velocity, ambulatory distance, stereotypic counts, vertical counts, ambulatory episodes, and total velocity. The decrease in vertical counts or rearing events was also observed in the original description of the Maryland model.²¹ There has been a human stroke study that correlated damage to the internal capsule with motor

deficits, which may explain the decrease in exploratory behavior we observed in our study and the DTI changes to the internal capsule.⁵⁴

Pearson's correlation analysis indicated a negative correlation with DTI measures and neurobehavioral assessment, MBP expression, and cytokine measures. The FA of splenium appeared to have the largest correlation with neurobehavioral results and MBP expression, whereas the LD and RD measures correlated with an increase in RANTES expression. Further studies are necessary to determine which pathways are altered following this particular mTBI and the potential mechanism behind these correlations.

There are different experimental models of TBI such as the fluid percussion and controlled cortical impact models that have been described as models of mTBI.^{15,18,20} Previous DTI studies have shown promise in detecting areas of axonal injury after TBI in various experimental models.^{5,6} Many of these injuries, even when classified as mTBI show lesions on conventional MRI. However, such lesions are seldom seen in human mTBI. Further, both the fluid percussion and controlled cortical impact models require craniotomy that alone may induce an inflammatory response and behavioral changes⁵⁵ that may make it clinically less relevant for human mTBI.

It would be interesting to compare our results with other published studies. Li and colleagues performed DTI on the Marmarou's impact acceleration model, where the force is delivered from the top of the skull.⁵⁶ These authors reported significant decrease in FA and LD in both the cc and ic after injury and with no significant difference in RD at 72 h post-injury.⁵⁶ Our DTI data on the Maryland mTBI model, which delivers a frontal impact acceleration injury, indicated a significant increase in FA and LD and a significant increase in RD in the scc and fi. Our results showed an increase in FA in the fi and ic. However, it should be pointed out that Li and associates measured FA on whole cc, whereas in our studies we subdivided cc into genu and splenium. Based on these studies it appears that brain white matter has different responses/vulnerabilities to not only the amount of force but also to the directionality of the force. The increase in FA post-injury is not totally surprising. For example, Bazarian and colleagues observed increased FA in the posterior cc in human mTBI compared with controls at 72 h post-injury.⁵⁷ Additional studies have also demonstrated an increase in FA in the cc and mesencephalon respectively of mTBI patients compared with controls.⁵⁸⁻⁶⁰ Kou and co-workers suggested that increased FA may be attributed to axonal swelling that occurs acutely after injury.⁶¹ Our study showed consistent FA increases in the regions analyzed. The early increase in FA has also been suggested to serve as a biomarker of poor outcome.⁹ A longitudinal study including earlier time points that may help follow the pathological changes using this experimental mTBI model to determine the significance of increased versus a decreased FA will need to be performed.

Conclusions

The major aim of this multi-modal study was to further characterize acute changes that occur following mTBI using the Maryland model, which reproduces many of the forces encountered by the human brain following motor vehicular or sports accidents. These results suggest that this model replicates many of the findings in human mTBI including the absence of anatomical lesions on conventional MRI and acute changes in the DTI parameters. Our study also indicated that some white matter tracts may be more vulnerable depending on the directionality of the force impacting

the brain compared with other impact models. Longitudinal mTBI studies are needed to determine the long-term consequences affecting learning, memory, anxiety, and depression. The longitudinal study would also determine if changes in behavior could be correlated to DTI measures in the brain. Such studies are underway.

Acknowledgments

The Translational Psychiatry Program (USA) is funded by the Department of Psychiatry and Behavioral Sciences, McGovern Medical School, The University of Texas Health Science Center at Houston (UTHealth). The 7T scanner purchase was supported by the NIH High End Instrumentation Grant (1 S10 RR17205-01) awarded to PAN.

Author Disclosure Statement

No competing financial interests exist.

References

- Faul, M., Xu, L., Wald, M., and Coronado, V. (2010). Traumatic Brain Injury in the United States: Emergency Department Visits, Hospitalizations and Deaths 2002–2006. Centers for Disease Control and Prevention, National Center for Injury Prevention and Control: Atlanta, GA.
- Gerberding, J.L., and Binder, S. (2003). Report to Congress on Mild Traumatic Brain Injury in the United States. Centers for Disease Control and Prevention (ed): Atlanta, GA.
- McCrorry, P., Meeuwisse, W., Johnston, K., Dvorak, J., Aubry, M., Molloy, M., and Cantu, R. (2009). Consensus Statement on Concussion in Sport: the 3rd International Conference on Concussion in Sport held in Zurich, November 2008. *Br. J. Sports Med.* 43, Suppl 1, i76–i90.
- Li, J., Li, X.Y., Feng, D.F., and Gu, L. (2011). Quantitative evaluation of microscopic injury with diffusion tensor imaging in a rat model of diffuse axonal injury. *Eur. J. Neurosci.* 33, 933–945.
- Mac Donald, C.L., Dikranian, K., Bayly, P., Holtzman, D., and Brody, D. (2007). Diffusion tensor imaging reliably detects experimental traumatic axonal injury and indicates approximate time of injury. *J. Neurosci.* 27, 11869–11876.
- Mac Donald, C.L., Dikranian, K., Song, S.K., Bayly, P.V., Holtzman, D.M., and Brody, D.L. (2007). Detection of traumatic axonal injury with diffusion tensor imaging in a mouse model of traumatic brain injury. *Exp. Neurol.* 205, 116–131.
- Petraglia, A.L., Dashnaw, M.L., Turner, R.C., and Bailes, J.E. (2014). Models of mild traumatic brain injury: translation of physiological and anatomic injury. *Neurosurgery* 75, Suppl 4, S34–S49.
- Petraglia, A.L., Plog, B.A., Dayawansa, S., Chen, M., Dashnaw, M.L., Czerniecka, K., Walker, C.T., Viterise, T., Hyrien, O., Iliff, J.J., Deane, R., Nedergaard, M., and Huang, J.H. (2014). The spectrum of neurobehavioral sequelae after repetitive mild traumatic brain injury: a novel mouse model of chronic traumatic encephalopathy. *J. Neurotrauma* 31, 1211–1224.
- Shenton, M.E., Hamoda, H.M., Schneiderman, J.S., Bouix, S., Pasternak, O., Rathi, Y., Vu, M.A., Purohit, M.P., Helmer, K., Koerte, I., Lin, A.P., Westin, C.F., Kikinis, R., Kubicki, M., Stern, R.A., and Zafonte, R. (2012). A review of magnetic resonance imaging and diffusion tensor imaging findings in mild traumatic brain injury. *Brain Imaging Behav.* 6, 137–192.
- Basser, P.J., and Jones, D.K. (2002). Diffusion-tensor MRI: theory, experimental design and data analysis—a technical review. *NMR Biomed.* 15, 456–467.
- Huisman, T.A., Schwamm, L.H., Schaefer, P.W., Koroshetz, W.J., Shetty-Alva, N., Ozsunar, Y., Wu, O., and Sorensen, A.G. (2004). Diffusion tensor imaging as potential biomarker of white matter injury in diffuse axonal injury. *AJNR. Am. J. Neuroradiol.* 25, 370–376.
- Lingsma, H.F., Yue, J.K., Maas, A.I., Steyerberg, E.W., Manley, G.T., Investigators, T.-T., Cooper, S.R., Dams-O'Connor, K., Gordon, W.A., Menon, D.K., Mukherjee, P., Okonkwo, D.O., Puccio, A.M., Schnyer, D.M., Valadka, A.B., Vassar, M.J. and Yuh, E.L. (2015). Outcome prediction after mild and complicated mild traumatic brain injury:

- external validation of existing models and identification of new predictors using the TRACK-TBI pilot study. *J. Neurotrauma* 32, 83–94.
13. Yuh, E.L., Cooper, S.R., Mukherjee, P., Yue, J.K., Lingsma, H.F., Gordon, W.A., Valadka, A.B., Okonkwo, D.O., Schnyer, D.M., Vassar, M.J., Maas, A.I., Manley, G.T., and Track-Tbi, I. (2014). Diffusion tensor imaging for outcome prediction in mild traumatic brain injury: a TRACK-TBI study. *J. Neurotrauma* 31, 1457–1477.
 14. Ghadiri, T., Sharifzadeh, M., Khodagholi, F., Modarres Mousavi, S.M., Hassanzadeh, G., Zarrindast, M.R., and Gorji, A. (2014). A novel traumatic brain injury model for induction of mild brain injury in rats. *J. Neurosci. Methods* 233, 18–27.
 15. Dixon, C.E., Lyeth, B.G., Povlishock, J.T., Findling, R.L., Hamm, R.J., Marmarou, A., Young, H.F., and Hayes, R.L. (1987). A fluid percussion model of experimental brain injury in the rat. *J. Neurosurg.* 67, 110–119.
 16. Gurkoff, G.G., Giza, C.C., and Hovda, D.A. (2006). Lateral fluid percussion injury in the developing rat causes an acute, mild behavioral dysfunction in the absence of significant cell death. *Brain Res.* 1077, 24–36.
 17. Yu, S., Kaneko, Y., Bae, E., Stahl, C.E., Wang, Y., van Loveren, H., Sanberg, P.R., and Borlongan, C.V. (2009). Severity of controlled cortical impact traumatic brain injury in rats and mice dictates degree of behavioral deficits. *Brain Res.* 1287, 157–163.
 18. Shapira, Y., Shohami, E., Sidi, A., Soffer, D., Freeman, S., and Cotev, S. (1988). Experimental closed head injury in rats: mechanical, pathophysiological, and neurologic properties. *Crit. Care Med.* 16, 258–265.
 19. Shohami, E., Shapira, Y., and Cotev, S. (1988). Experimental closed head injury in rats: prostaglandin production in a noninjured zone. *Neurosurgery* 22, 859–863.
 20. Marmarou, A., Foda, M.A., van den Brink, W., Campbell, J., Kita, H., and Demetriadou, K. (1994). A new model of diffuse brain injury in rats. Part I: Pathophysiology and biomechanics. *J. Neurosurg.* 80, 291–300.
 21. Kilbourne, M., Kuehn, R., Tosun, C., Caridi, J., Keledjian, K., Bochicchio, G., Scalea, T., Gerzanich, V., and Simard, J.M. (2009). Novel model of frontal impact closed head injury in the rat. *J. Neurotrauma* 26, 2233–2243.
 22. Council, N.R. (2011). *Guide for the Care and Use of Laboratory Animals*, 8th ed. The National Academies Press: Washington, DC.
 23. Narayana, P.A., Herrera, J.J., Bockhorst, K.H., Esparza-Coss, E., Xia, Y., Steinberg, J.L., and Moeller, F.G. (2014). Chronic cocaine administration causes extensive white matter damage in brain: diffusion tensor imaging and immunohistochemistry studies. *Psychiatry Res.* 221, 220–230.
 24. Madi, S., Hasan, K.M., and Narayana, P.A. (2005). Diffusion tensor imaging of in vivo and excised rat spinal cord at 7 T with an icosahedral encoding scheme. *Magn. Reson. Med.* 53, 118–125.
 25. Narayana, P.A., Ahobila-Vajjula, P., Ramu, J., Herrera, J., Steinberg, J.L., and Moeller, F.G. (2009). Diffusion tensor imaging of cocaine-treated rodents. *Psychiatry Res.* 171, 242–251.
 26. Hahn, K., Prigarin, S., and Hasan, K. (2005). The feasibility of diffusion tensor imaging for the human brain at 1 mm³ resolution. *Proc. Intl. Soc. Mag. Reson. Med.* 13, 161.
 27. Woods, R.P., Grafton, S.T., Holmes, C.J., Cherry, S.R., and Mazziotta, J.C. (1998). Automated image registration: I. General methods and intrasubject, intramodality validation. *J. Comput. Assist. Tomogr.* 22, 139–152.
 28. Smith, S.M., Jenkinson, M., Woolrich, M.W., Beckmann, C.F., Behrens, T.E., Johansen-Berg, H., Bannister, P.R., De Luca, M., Drobnjak, I., Flitney, D.E., Niazy, R.K., Saunders, J., Vickers, J., Zhang, Y., De Stefano, N., Brady, J.M., and Matthews, P.M. (2004). Advances in functional and structural MR image analysis and implementation as FSL. *Neuroimage* 23, Suppl 1, S208–S219.
 29. Herrera, J.J., Chacko, T., and Narayana, P.A. (2008). Histological correlation of diffusion tensor imaging metrics in experimental spinal cord injury. *J. Neurosci. Res.* 86, 443–447.
 30. Metz, G.A., Merkle, D., Dietz, V., Schwab, M.E., and Fouad, K. (2000). Efficient testing of motor function in spinal cord injured rats. *Brain Res.* 883, 165–177.
 31. Rutgers, D.R., Toulgoat, F., Cazejust, J., Fillard, P., Lasjaunias, P., and Ducreux, D. (2008). White matter abnormalities in mild traumatic brain injury: a diffusion tensor imaging study. *AJNR. Am. J. Neuroradiol.* 29, 514–519.
 32. Narayana, P.A., Yu, X., Hasan, K.M., Wilde, E.A., Levin, H.S., Hunter, J.V., Miller, E.R., Patel, V.K., Robertson, C.S., and McCarthy, J.J. (2015). Multi-modal MRI of mild traumatic brain injury. *Neuroimage Clin.* 7, 87–97.
 33. Hemphill, M.A., Dauth, S., Yu, C.J., Dabiri, B.E., and Parker, K.K. (2015). Traumatic brain injury and the neuronal microenvironment: a potential role for neuropathological mechanotransduction. *Neuron* 85, 1177–1192.
 34. Sharp, D.J., and Ham, T.E. (2011). Investigating white matter injury after mild traumatic brain injury. *Curr. Opin. Neurol.* 24, 558–563.
 35. Song, S.K., Sun, S.W., Ramsbottom, M.J., Chang, C., Russell, J., and Cross, A.H. (2002). Demyelination revealed through MRI as increased radial (but unchanged axial) diffusion of water. *Neuroimage* 17, 1429–1436.
 36. Zhang, J., Jones, M., DeBoy, C.A., Reich, D.S., Farrell, J.A., Hoffman, P.N., Griffin, J.W., Sheikh, K.A., Miller, M.I., Mori, S., and Calabresi, P.A. (2009). Diffusion tensor magnetic resonance imaging of Wallerian degeneration in rat spinal cord after dorsal root axotomy. *J. Neurosci.* 29, 3160–3171.
 37. Song, S.K., Yoshino, J., Le, T.Q., Lin, S.J., Sun, S.W., Cross, A.H., and Armstrong, R.C. (2005). Demyelination increases radial diffusivity in corpus callosum of mouse brain. *Neuroimage* 26, 132–140.
 38. Beaulieu, C. (2002). The basis of anisotropic water diffusion in the nervous system—a technical review. *NMR Biomed.* 15, 435–455.
 39. Redell, J.B., Moore, A.N., Grill, R.J., Johnson, D., Zhao, J., Liu, Y., and Dash, P.K. (2013). Analysis of functional pathways altered after mild traumatic brain injury. *J. Neurotrauma* 30, 752–764.
 40. Derecki, N.C., Cardani, A.N., Yang, C.H., Quinnes, K.M., Crihfield, A., Lynch, K.R., and Kipnis, J. (2010). Regulation of learning and memory by meningeal immunity: a key role for IL-4. *J. Exp. Med.* 207, 1067–1080.
 41. Zhou, L., and Shine, H.D. (2003). Neurotrophic factors expressed in both cortex and spinal cord induce axonal plasticity after spinal cord injury. *J. Neurosci. Res.* 74, 221–226.
 42. Choy, K.H., de Visser, Y., Nichols, N.R., and van den Buuse, M. (2008). Combined neonatal stress and young-adult glucocorticoid stimulation in rats reduce BDNF expression in hippocampus: effects on learning and memory. *Hippocampus* 18, 655–667.
 43. Hall, J., Thomas, K.L., and Everitt, B.J. (2000). Rapid and selective induction of BDNF expression in the hippocampus during contextual learning. *Nat. Neurosci.* 3, 533–535.
 44. Butovsky, O., Talpalar, A.E., Ben-Yaakov, K., and Schwartz, M. (2005). Activation of microglia by aggregated beta-amyloid or lipopolysaccharide impairs MHC-II expression and renders them cytotoxic whereas IFN-gamma and IL-4 render them protective. *Mol. Cell. Neurosci.* 29, 381–393.
 45. Baratz, R., Tweedie, D., Wang, J.Y., Rubovitch, V., Luo, W., Hoffer, B.J., Greig, N.H., and Pick, C.G. (2015). Transiently lowering tumor necrosis factor- α synthesis ameliorates neuronal cell loss and cognitive impairments induced by minimal traumatic brain injury in mice. *J. Neuroinflammation* 12, 45.
 46. Shohami, E., Novikov, M., Bass, R., Yamin, A., and Gallily, R. (1994). Closed head injury triggers early production of TNF α and IL-6 by brain tissue. *J. Cereb. Blood Flow Metab.* 14, 615–619.
 47. Taupin, V., Toulmond, S., Serrano, A., Benavides, J., and Zavala, F. (1993). Increase in IL-6, IL-1 and TNF levels in rat brain following traumatic lesion. Influence of pre- and post-traumatic treatment with Ro5 4864, a peripheral-type (p site) benzodiazepine ligand. *J. Neuroimmunol.* 42, 177–185.
 48. Cammer, W. (2000). Effects of TNF α on immature and mature oligodendrocytes and their progenitors in vitro. *Brain Res.* 864, 213–219.
 49. Kita, T., Tanaka, T., Tanaka, N., and Kinoshita, Y. (2000). The role of tumor necrosis factor- α in diffuse axonal injury following fluid-percussive brain injury in rats. *Int. J. Legal Med.* 113, 221–228.
 50. Hendrzak, J.A., and Brunda, M.J. (1995). Interleukin-12. Biologic activity, therapeutic utility, and role in disease. *Lab Invest.* 72, 619–637.
 51. Trinchieri, G. (1995). Interleukin-12: a proinflammatory cytokine with immunoregulatory functions that bridge innate resistance and antigen-specific adaptive immunity. *Annu. Rev. Immunol.* 13, 251–276.
 52. Trinchieri, G., and Scott, P. (1994). The role of interleukin 12 in the immune response, disease and therapy. *Immunol. Today* 15, 460–463.
 53. Stahel, P.F., Kossmann, T., Joller, H., Trentz, O., and Morganti-Kossmann, M.C. (1998). Increased interleukin-12 levels in human cerebrospinal fluid following severe head trauma. *Neurosci. Lett.* 249, 123–126.

54. Pendlebury, S.T., Blamire, A.M., Lee, M.A., Styles, P., and Matthews, P.M. (1999). Axonal injury in the internal capsule correlates with motor impairment after stroke. *Stroke* 30, 956–962.
55. Cole, J.T., Yarnell, A., Kean, W.S., Gold, E., Lewis, B., Ren, M., McMullen, D.C., Jacobowitz, D.M., Pollard, H.B., O'Neill, J.T., Grunberg, N.E., Dalgard, C.L., Frank, J.A., and Watson, W.D. (2011). Craniotomy: true sham for traumatic brain injury, or a sham of a sham? *J. Neurotrauma* 28, 359–369.
56. Li, S., Sun, Y., Shan, D., Feng, B., Xing, J., Duan, Y., Dai, J., Lei, H., and Zhou, Y. (2013). Temporal profiles of axonal injury following impact acceleration traumatic brain injury in rats—a comparative study with diffusion tensor imaging and morphological analysis. *Int. J. Legal Med.* 127, 159–167.
57. Bazarian, J.J., Zhong, J., Blyth, B., Zhu, T., Kavcic, V., and Peterson, D. (2007). Diffusion tensor imaging detects clinically important axonal damage after mild traumatic brain injury: a pilot study. *J. Neurotrauma* 24, 1447–1459.
58. Hartikainen, K.M., Waljas, M., Isoviita, T., Dastidar, P., Liimatainen, S., Solbakk, A.K., Ogawa, K.H., Soimakallio, S., Ylinen, A., and Ohman, J. (2010). Persistent symptoms in mild to moderate traumatic brain injury associated with executive dysfunction. *J. Clin. Exp. Neuropsychol.* 32, 767–774.
59. Henry, L.C., Tremblay, J., Tremblay, S., Lee, A., Brun, C., Lepore, N., Theoret, H., Ellemberg, D., and Lassonde, M. (2011). Acute and chronic changes in diffusivity measures after sports concussion. *J. Neurotrauma* 28, 2049–2059.
60. Mayer, A.R., Ling, J., Mannell, M.V., Gasparovic, C., Phillips, J.P., Doezeza, D., Reichard, R., and Yeo, R.A. (2010). A prospective diffusion tensor imaging study in mild traumatic brain injury. *Neurology* 74, 643–650.
61. Kou, Z., Wu, Z., Tong, K.A., Holshouser, B., Benson, R.R., Hu, J., and Haacke, E.M. (2010). The role of advanced MR imaging findings as biomarkers of traumatic brain injury. *J. Head Trauma Rehabil.* 25, 267–282.

Address correspondence to:

Juan J. Herrera, PhD

Department of Diagnostic and Interventional Imaging

The University of Texas Medical School at Houston

6431 Fannin, MSE R102F

Houston, TX 77030

E-mail: Juan.Herrera@uth.tmc.edu